Proceedings World Geothermal Congress 2020+1
Reykjavik, Iceland, April - October 2021

Soft-stimulating Injection Procedures to Improve Geothermal Reservoir Performance

Laura J. Wasch, Hester E. Dijkstra and Mariëlle K. Koenen

TNO, Princetonlaan 6, 3584 CB Utrecht, The Netherlands

Laura.wasch@tno.nl

Keywords: Injectivity stimulation, scaling, reservoir geochemistry, numerical modelling, batch experiments

ABSTRACT

Geothermal plants may face a large variety of operational problems caused by scaling, particle clogging and inefficient injection strategies. Flow obstruction is well known in surface facilities and wells but difficult to observe and mitigate in the reservoir. A key challenge in geothermal energy production is the decline of injectivity over time. Rather than diverting to harsh reservoir fracking to improve injectivity we aim to develop gentle and low-cost techniques to overcome low injectivity. The technologies include *thermal* and *CO_2-(re)injection* soft-stimulating injection procedures. Cooling of water and gas exsolution during geothermal energy production disturbs the chemical equilibrium of the water, frequently causing scaling (mineral precipitation). Alternatively, similar chemical and physical changes of the produced water may result in mineral dissolution, improving reservoir flow properties. Mineral (e.g. calcite) dissolution could be stimulated by both cooling and increasing the dissolved CO_2 content. The effects of thermal and CO_2-(re)injection soft-stimulation on the geothermal reservoir are assessed with reactive transport simulations with TOUGHREACT software and laboratory batch experiments. Experiments are performed with both the produced water and the original cuttings of a Dutch geothermal well targeting the Delft sandstone. A field-scale model is developed using site data on water, gas and rock compositions, pressure and temperature conditions and flow properties. Ultimately, optimization of production and injection procedures is crucial for good flow and injectivity would create more energy output and improve cost-effectiveness.

1. INTRODUCTION

The Dutch government has set the ambitious goal to reduce CO_2 emissions in the Netherlands by 55% in 2030. To achieve this goal, investment is required in the development of CO_2 reducing technologies such as carbon capture and storage (CCS), wind and solar energy and geothermal energy. A large part of the energy consumed in the Netherlands is used for heating (Veldkamp and Boxem, 2015), making geothermal energy a very relevant technology for the Dutch energy mix in the future. With 14 active geothermal doublets in 2017, the geothermal sector in the Netherlands is still small and relatively undeveloped, and the available knowledge is limited and often case specific (Staatstoezicht op de Mijnen, 2017). Geothermal operators in the Netherlands face operational problems caused by unexpected low permeabilities, or reduction of injectivity over time due to scaling, corrosion and clogging (Schreiber et al., 2016, Veldkamp and Boxem, 2015). In the Horizon 2020 project PERFORM, these processes are being investigated and cost-effective solutions are researched to support operators in reducing operational costs and improving the geothermal business case. Dissemination of the project results with the relevant stakeholders will boost sustainable geothermal energy exploitation.

Operations with an initial proper injectivity, often face deterioration of injectivity over time. Blockage of the reservoir pore space reduces the permeability and hence the injectivity of the well (Ungemach, 2003, Blöcher et al., 2016, Gallup, 2009, Heshauss et al. 2013). Different materials could be responsible for clogging the pores, including reservoir fines, corrosion products, scale particles or even in situ precipitating minerals induced by chemical interaction between the injected brine and reservoir (Ungemach, 2003, Boch et al, 2017). Mineral precipitation (scaling) is an issue that occurs in geothermal wells all over Europe (Schreiber et al., 2016). Depending on the pressure and temperature conditions, the host rock and formation water chemistry, different types of scales can be formed. These include carbonates, iron oxides, Ba-, Fe- and Sr-sulphates, and clay and lead precipitates (Boch et al., 2017, Holmslykke, 2017, Orywall, 2017, Regenspurg et al., 2010). Although scaling is mainly reported in surface installations and wells, it is important to consider the possibility of supersaturation and (kinetically delayed) precipitation of these scaling minerals in the reservoir itself causing injectivity issues (Ungemach et al., 2003).

In the case of injectivity reduction over time or when an operator is negatively surprised by a low permeability of the targeted formation, the reservoir rock can be stimulated. Most practiced stimulation methods involve acid injection or fracking. These stimulation methods are often costly and insufficient, asking for more low-cost, environmentally friendly and soft-stimulating strategies for reservoir improvement. Soft thermal or chemical stimulation could be a low-cost technology to enhance the injectivity of the reservoir. The low temperature of the injection water can induce carbonate dissolution (thermal stimulation) with the benefit of increasing the energy extracted from geothermal water. The addition of dissolved CO_2 to the injection water will reduce the pH which may cause additional dissolution of reservoir (carbonate) minerals, increasing porosity and reservoir flow. CO_2 is often already present in Dutch geothermal reservoirs and many doublets show gas release from production water at the surface due to the pressure decrease and corresponding gas solubility decrease (Wasch 2014). Re-injecting the CO_2 from the produced geothermal water, or even maximizing CO_2 co-injection in the injected water could stimulate the injectivity of low permeable formations and support CO_2 emission reductions at the same time. For example, experiments with CO_2-saturated brine on Rotliegendes sandstone show a permeability increase by a factor of two due to the dissolution of anhydrite and calcite (Huq et al., 2015). This indicates the potential of increasing reservoir permeability by injecting a CO_2 enriched fluid.

The effect of soft chemical stimulation with dissolved CO_2 and thermal stimulation on reservoir flow will be investigated by reactive transport modelling with TOUGHREACT software. The models will be validated with batch experiments at reservoir conditions using well cuttings and the actual geothermal water. This enables us to capture the full chemical complexity of the system.

2. GEOLOGICAL BACKGROUND AND RESERVOIR CHARACTERISTICS

The doublet used as case study targets the Delft Sandstone member in the Westland area, which is located in the West Netherlands Basin (WNB). This basin is a transtensional basin in the southwest of the Netherlands. It is composed of structural highs and lows with a NW-SE orientation, formed by rifting occurring from the late Jurassic to the Early Cretaceous (Van Balen et al., 1999). During this period syntectonic deposition of fluvial material occurred, forming the lower part of the Delft sandstone member. When rifting slowed, the basin started to subside which resulted in marine transgression. This led to a transition from fluvial depositional environment to a marine environment. In the Late Cretaceous the Laramide compressional phase caused inversion and uplift in the basin with reactivation of many faults (Donselaar et al. 2015). Inversion caused uplift of the former depocenters subsequently accompanied by erosion (Van Balen et al. 1999).

The Delft sandstone member can be divided into three units (Donselaar et al., 2015). The upper and lower unit consisting of fluvial sandstones. The middle member consisting of claystone and siltstone rich layers. Deposition of the lower unit is characterized by loosely stacked fluvial sandstone bodies, which are highly heterogeneous and have low a connectivity. The middle unit was deposited during sea-level rise, which lead to the deposition of fine-grained floodplain and swamp sediments. When the rate of sea level rise decreased, unit three was deposited as fluvial sandstones. These three units have very different permeabilities (Donselaar et al., 2015). The permeability of unit one increases from 90 mD at the base to 295 mD at the top of the unit, with an average porosity of 19%. Unit three has a permeability that varies between 725 mD and 1130 mD with the highest permeability at the base and an average porosity of 30%. Unit two consist of very fine-grained silts and clays and has a low porosity and permeability. We assume that unit 1 and 3 mainly contribute to water production and water injection and hence focused on the chemical and reservoir properties of these units.

The Delft sandstone was characterized by mineralogical (XRD) analyses of the cuttings of different wells (table 1). All samples have quartz as the main component, variable calcite from <1 wt.% to 39.3 wt.% and contain clays. Minor components are iron/magnesium carbonates and iron/titanium oxides. Measured salt is excluded since salt is attributed to incomplete washing of the cuttings. The weight percentages of table 1 can be used to calculate the volume fraction of calcite in the rock. The maximum measured calcite is 39.3%, which represents a volume of 39.0% and hence a potential maximum porosity increase upon full calcite dissolution of 39%. For the HON-GT-01 well, the volume of calcite and hence the potential porosity increase is 13.43% (2580 m sample) and 3.25% (2620 m sample). The potential for soft stimulation by calcite dissolution is hence variable but significant.

Table 1: Mineralogical composition of Delft sandstone member cutting samples of several wells.

Well, sample depth (m)	**HAG-GT-01**	**HAG-GT-01**	**HAG-GT-02**	**PNA-GT-01**	**PNA-GT-02**	**PNA-GT-02**	**HON-GT-01**	**HON-GT-01**	**HON-GT-02**	**HON-GT-02**
Mineral - formula	2611	2661	2220	2800	2660	2710	2580	2620	2650	2750
Quartz - SiO_2	75.2	86	57.7	73.9	92.3	89.2	81.3	89.4	83.5	70.4
Calcite - $CaCO_3$	6.2	5.6	39.3	0.9	0.3	0.3	13.6	3.3	0.6	4.8
Mg-Calcite - $(Ca,Mg)CO_3$	-	-	-	0.3	-	-	-	-	-	-
Ankerite - $Ca(Fe,Mg,Mn)(CO_3)_2$	-	-	-	-	-	0.1	-	-	-	-
Siderite - $FeCO_3$	0.6	-	-	3.5	0.2	2.1	0.5	0.6	0.5	0.1
Pyrite - FeS_2	0.5	0.3	0.2	0.5	0.1	0.1	0.1	0.1	0.2	0.1
Hematite - Fe_2O_3	-	-	0.1	-	-	-	-	-	-	-
Anatase - TiO_2	0.4	0.3	0.1	0.4	0.3	0.3	0.2	0.2	0.4	0.4
Rutile - TiO_2	0.2	0.1	0.1	0.3	0.2	0.2	0.1	0.1	0.2	0.2
Kaolinite - $Al_2Si_2O_5(OH)_4$	5.7	2.9	1.3	6.9	2.6	2.9	2.4	2.6	5.3	6.6
Chlorite - $(Fe,Mg,Fe)_5 Al(Si_3Al)O_{10}(OH,O)_8$	-	-	0.1	0.1	-	-	-	-	-	-
2:1 layer silicate - $(Al,Mg,Fe)_2 (Si,Al)_4O_{10} [(OH)_2,(H_2O)]$	8.6	4.8	1.1	13.1	3.9	4.9	1.7	3.6	9.0	9.0

3. METHODS AND MODEL INPUT

3.1 Experimental setup

The experiment was designed to study the influence of injection temperature and co-injected CO_2 on the reservoir rock. In figure 1, a simplified version of the experimental setup is shown. The setup consists of a stainless-steel autoclave which can hold one litre of

fluid and resists pressures up to 600 bar. The sample is placed in a Teflon beaker inside the vessel. Before the start of the experiment, the vessel is flushed with nitrogen to remove the oxygen in the vessel. The brine used in the experiment is sampled directly from the geothermal system, just after the brine passed the heat exchanger at conditions of ~ 40°C and 3-4 bar. To prevent the CO_2 in the brine from degassing completely, the operator keeps the system pressurized at 3 to 4 bar. To retain this pressure, the autoclave was filled until the valve opened at a pressure of 3.5 bar and the level meter indicated that the desired water level was reached. After transportation to the laboratory, the autoclave was slowly pressurized to 50 bar with nitrogen. The brine was continuously stirred during the experiment to represent flow conditions. Water samples were taken with an outlet before opening and fully depressurizing the system. This was done to minimize changes to the water due to water-rock interaction under atmospheric conditions. Experiments were run at ~40 °C and ~20 °C and will be run with different levels of CO_2.

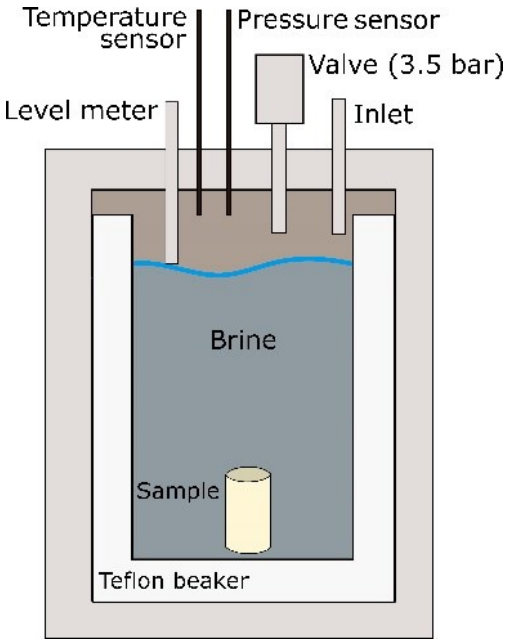

Figure 1: The batch experimental setup showing stainless steel autoclave.

3.2 Reactive transport simulator

A reactive transport model was developed using TOUGHREACT software version 3.32 (Xu et al., 2006). The simulator couples reactive chemistry to the TOUGH2 simulator of multiphase and multicomponent fluid flow in porous and fractured media (Pruess et al., 1999). We used the ECO2N fluid property module which includes the thermodynamic and thermophysical properties of H_2O - NaCl - CO_2 mixtures (Pruess, 2005). The ECO2N equation of state covers fluid properties for conditions of 10 °C < T < 300 °C, P < 600 bar, and salinity up to halite saturation. Note that besides water only one gas can be included in the simulator. Since CH_4 is considered inert with respect to inorganic mineral reactions, only CO_2 was included. For chemical simulations the thermodynamic database Thermoddem was used, version of 6 July 2017 (Blanc et al., 2012). The reaction of minerals is kinetically controlled using a rate expression of Lasaga et al. (1994). Mineral kinetics are included using the reaction rates of Palandri and Kharaka (2004).

The TOUGH2 pre- and post-processor Petrasim was used to create a polygonal mesh. The mesh dimensions are 1.5 by 3 km with a simplified geology of one layer with a top at 2300 m and a base at 2700 m. The two wells are 1.5 km apart. An area of 1250 m² was chosen as maximum cell size. For the minimum cell area near-well, a value of 0.1 m^2 was selected (yielding a ~40 cm cell diameter). With these input values, a mesh of 3509 cells was created. The boundary conditions are assumed to be closed. The rock is initially homogeneous with a porosity of 18% and a permeability of 7.5E-13 m² (750 mD). Water-rock reactions change the volume of minerals and hence the porosity. Porosity changes are calculated using mineral the specific molar volumes included in the thermodynamic database. Based on the porosity, the permeability is altered. We used the porosity-permeability relationship of Verma and Pruess (1988). With a critical porosity of 85% of the initial porosity and a power law component of 4 (formula 1). These values are average values used for porous media (Hommel et al., 2018).

$$\frac{k}{ki_i} = \left(\frac{\phi - \phi_c}{\phi_i - \phi_c}\right)^n \quad (1)$$

Where k is the permeability, ki the initial permeability, φ the porosity, φi the initial porosity, φc the critical porosity below which the permeability goes to zero, and n is a power law exponent.

The initial reservoir pressure is 255 bar with a temperature of 88 °C. The base case injection temperature is 30 °C. The doublet co-produces CH_4 and CO_2 with the water. The surface installation contains a gas separator tank which is kept at a pressure of 4 bar. At this pressure most of the methane is exsolved, - which is used as an additional energy source - but still a fraction of CO_2 is kept in solution. Keeping an amount of CO_2 in solution is required to limit the pH increase and prevent calcite scaling (Alt-Epping et al., 2012, Wasch, 2014). Two values are available for CO_2 content, one measured of the gas separated in the separator tank and one recalculated for the total gas. The recalculation takes into account that at 4 bar, the CO_2 and CH_4 fractions are different than when degassed at 1 bar due to the pressure dependent solubility of CO_2. The CO_2 concentrations in the produced and injected water can be calculated using the measured gas and water compositions (table 2). The calculated initial amount of CO_2 in the reservoir is 2.29E-02 mol/l, which is the measured dissolved CO_2 (1.43E-02 mol/l) plus the total separated CO_2 at standard conditions (8.61E-03 mol/l).

This yields a dissolved mass fraction of CO_2 of 9.05E-04 (=n MCO_2/(1000 + m MNaCl + n MCO_2)) as used in TOUGH2. For re-injection, a CO_2 concentration value of 1.938E-02 mol/l was used, which is the CO_2 concentration in the reservoir (2.29E-02 mol/l) minus the separated CO_2 (3.57E-03 mol/l). We used a salinity in TOUGH2 with an Xs value of 0.1 (Xs=m*MNaCl/(1000+m*MNaCl)), based on a measurement of 38800 mg/L Na^+ and 75710 mg/L Cl^-. With a simplified constant well flow of 150 m^3/h water, the injected masses were calculated (table 3). Injection is defined for each component of the fluid separately while production is defined by a mass equal to the sum of the injected components.

The mineralogy of sample HON-GT-01 2580 m depth is selected for the reservoir composition and contains 13.6 wt.% calcite (table 1). The type of clay was not analysed with XRD and smectite was selected since it is close to equilibrium with the formation water (i.e. changes the compositions the little upon equilibration). The total mineralogy as used in TOUGHREACT is listed in table 4. The measured water composition from HON-GT-01 well geothermal water is initialized in TOUGHREACT with the measured exsolved CO_2 at reservoir conditions. The water composition obtained after equilibration with the reservoir minerals is listed in table 5.

Table 2: Data and calculations for the exsolved and dissolved CO_2.

	Nm^3 (gas)/ Nm^3 (fluid)	**molar volume (l/mol @ 0 °C, 1 atm)**	**Total gas (mol /l)**	**CO_2 fraction (mol %)**	**CO_2 (mol /l)**
Gas separated @ 4bar	0.896	22.414	3.998E-02	8.93	3.57E-03
Total gas exsolved	1.01	22.414	4.506E-02	19.1	8.61E-03

Table 3: Injection and production data.

	Component	**Rate (kg/s)**	**Enthalpy (J/kg)**
Injection	Water	41.67	148800
	Salt	4.771	-
	CO_2	0.036	252100
Production	Mass	-46.477	-

Table 4: Reservoir mineralogy.

Mineral	**quartz**	**calcite**	**siderite**	**pyrite**	**kaolinite**	**smectite(MX80)**
Formula	SiO_2	$CaCO_3$	$FeCO_3$	FeS_2	$Al_2Si_2O_5(OH)_4$	$Na_{0.409}K_{0.024}Ca_{0.009}(Si_{3.738}Al_{0.262})(Al_{1.598}Mg_{0.214}Fe_{0.208})O_{10}(OH)_2$
Volume Fraction	0.616	0.101	2.54E-03	4.0E-04	1.85E-02	1.22E-02

Table 5: Equilibrated water composition.

Element	**H^+**	**Ca^{+2}**	**Mg^{+2}**	**Na^+**	**K^+**	**H_4SiO_4**	**HCO_3^-**	**SO_4^{-2}**	**Al^{+3}**	**Cl^-**	**Ba^{+2}**	**Fe^{+2}**
Concentration (mol/l)	1.19E-02	0.175	4.61E-02	1.92	1.94E-02	7.41E-04	1.86E-02	7.06E-03	2.34E-08	2.37	2.11E-05	1.47E-03

4. RESULTS

4.1 Batch experiment of reservoir base case reactions upon cooling

A batch experiment with Delft sandstone cuttings was run for 1 week at 30 °C using the geothermal water sampled from the actual well. The mineralogy of the reacted cuttings is compared to the composition of a subsample (table 6). The experiment shows a reduction in the calcite content indicating calcite dissolution. The measured water composition before and after the experiment also shows an increase in calcium concentration of 300 mg/l. The increase in iron phases is linked to oxygenation of the water due to a leak in the autoclave, this also lays additional uncertainty on the experimental results. The difference in quartz and rutile is not expected for the experiment and also does not fit with the water composition, possibly indicating heterogeneity of the subsamples. The shown increase in clay minerals may indicate that clays could be of importance as reservoir scaling minerals. However, the experiment is currently being duplicated with a core plug to reduce the level of uncertainty. No barite was measured by XRD, but SEM investigation did show a Sr containing mineral. The change in water composition was inconclusive for barium but did show a decrease in strontium of 30 mg/l.

Table 6: Mineralogy of the cuttings before and after the experiment

Mineral	Quartz	Calcite	Siderite	Pyrite	Hematite	Anatase /Rutile	Kaolinite	Chlorite	2:1 layer silicate
Initial wt.%	81.3	13.6	0.5	0.1	-	0.3	2.4	-	1.7
Experiment wt.%	78.4	6.7	1.4	0.3	0.2	0.6	5.8	0.3	6.5

4.2 TOUGHREACT modelling of thermal reservoir stimulation

4.2.1 Thermal stimulation scenarios

Scenarios of changing injection temperature were run to investigate the chemical effects in the reservoir and corresponding impact on injectivity. The simulations are aimed at finding an optimum of increased heat extraction, enhanced stimulation of the reservoir (mineral dissolution) and low reservoir mineral precipitation. The injection water is based on the geothermal water with CO_2 concentration at 4 bar. Three scenarios were run at injection temperatures of 20°C, 30°C (base case) and 40°C (table 7). The temperature of the injected fluid is changed by adapting the enthalpy for water and CO_2. Note that the effect of changing pressure during injection on the (pressure dependent) enthalpy was not considered. Results are compared after 7 years. This is the operational lifetime of the doublet, ignoring potential downtime due to maintenance.

Table 7. Enthalpy values of injected water and CO_2 for different temperature scenarios.

Injection temperature	30 °C	40 °C	20 °C
Enthalpy water (J/kg)	148793	107643	189982
Enthalpy CO_2 (J/kg)	252060	232230	272360

4.2.1 Model results for the thermal stimulation scenarios

After 7 years of production and injection, the temperature front in the base case reaches about 250 m into the reservoir from the injection well (figure 2, upper). For the different thermal scenarios, the temperature gradient is compared along a transect between the injection and production well (figure 3a). This clearly shows the different injection temperatures near-well and an equal progression of the temperature fronts. The pressure is different for the different scenarios although all show the same characteristics of a low pressure near the production well and relatively high pressure near the injection well (figure 3b). For all three scenarios, the injection of water that is colder than the reservoir temperature causes a general pressure decrease in the reservoir. This is due to the higher density and reduced volume of the cooled injection water (figure 2, upper). This effect is also reflected in the pressure difference between the scenarios, with the lowest pressure for the lowest temperature (figure 3b). Furthermore, gas separation at 4 bar extracts mass from the system also contributing to pressure decreases in the reservoir.

Injection of cold water in the reservoir induces dissolution of the calcite in the rock formation. Colder temperatures yield increased progression of calcite dissolution, but the differences for the thermal scenarios are small (figure 3c). The fast reaction of calcite causes a sharp front at about 2 m into the reservoir. Siderite both precipitates and dissolves in the cooled zone (figure 3d). Siderite shows dissolution near-well, where calcite is completely dissolved, and siderite is used next to buffer the low pH of the injected solution. Precipitation occurs further reservoir inwards as dissolved species are transported away from the dissolution zone and the saturation index of siderite becomes positive. Siderite precipitation is enhanced at higher temperatures and hence results in a higher pH (figure 3e). The exhaustion of buffering carbonates in the 2 m around the injection well is represented in a pH drop near well. Other minerals showing a tendency to precipitate are smectite and kaolinite, however the amounts are very small (<0.01% volume fraction, results not shown). Barite also precipitates in small volumes but does form even beyond the cooled zone (figure 3f). The most significant reaction with respect to the porosity and permeability change, is calcite dissolution. This results in a porosity increase from 19 % to 29 % (figure 3g) and a permeability increase from 7.40E-13 m2 (750 mD) to 3.75E-12 (3.75 D) (figure 3h). Hence the permeability enhancement near-well is potentially significant but appears not very different for 20, 30 and 40 °C injection.

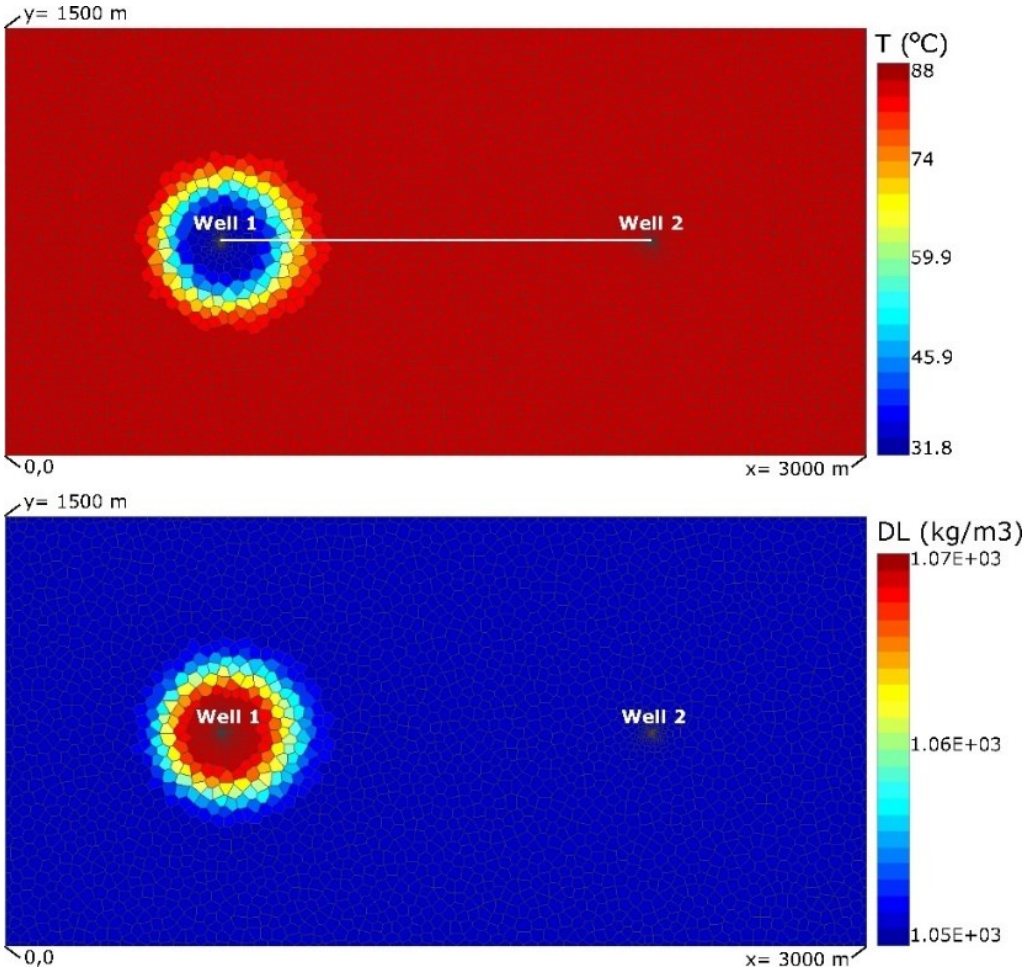

Figure 2: The base case simulation results after 7 years of production and injection for temperature (upper) and the density of the liquid (lower). The two wells with smaller cells around are indicated.

4.3 TOUGHREACT modelling of soft reservoir stimulation with dissolved CO_2

4.3.1 Dissolved CO_2 scenarios

Four scenarios were defined to study the effect of injecting different CO_2 concentrations on reservoir injectivity and pressure/temperature response (table 8). The base case simulation, as discussed in the previous section, is based on degassing of the production fluid at 4 bar which reduces the CO_2 concentration of the fluid. The second scenario of CO_2 re-injection assumes that all produced gas is re-injected, which could be done by re-injecting the separated CO_2 or by not degassing at the top side. The latter represents the conditions when the pressure in the system is high enough to prevent any CO_2 from coming out of solution. A third scenario was defined by re-injecting all produced gases, both CO_2 and CH_4 (in CO_2-equivalent). This scenario represents re-injecting the CO_2 degassed in the separator tank as well as the CO_2 liberated from burning the produced CH_4. Scenarios two and three would prevent emissions of greenhouse gasses, representing carbon-neutral geothermal energy production. For the fourth scenario, CO_2 was dissolved up to brine saturation level at 200 bar and 30°C. In this case, additional CO_2 is added to the reservoir with the objective of maximizing CO_2 emission reduction and contributing to CO_2 storage. The scenarios all have different masses of dissolved CO_2 injection (table 8). Dissolving different levels of CO_2 affects the chemistry of the injected waters. To include this affect, the water compositions are initialized with amounts of CO_2 representing the injection rates (table 8).

Table 8: Four soft stimulation scenarios with increasing CO_2 injection rates.

Scenario	CO_2 injection rate (kg/s)	Dissolved CO_2, HCO_3^- (mol/l)
1. Base case (CO_2 degassing @ 4 bar)	0.036	1.86E-02
2. CO_2 re-injection	0.042	2.48E-02
3. CH_4-used CO_2 injection	0.098	5.36E-02
4. Maximized CO_2 co-injection	1.834	5.57E-01

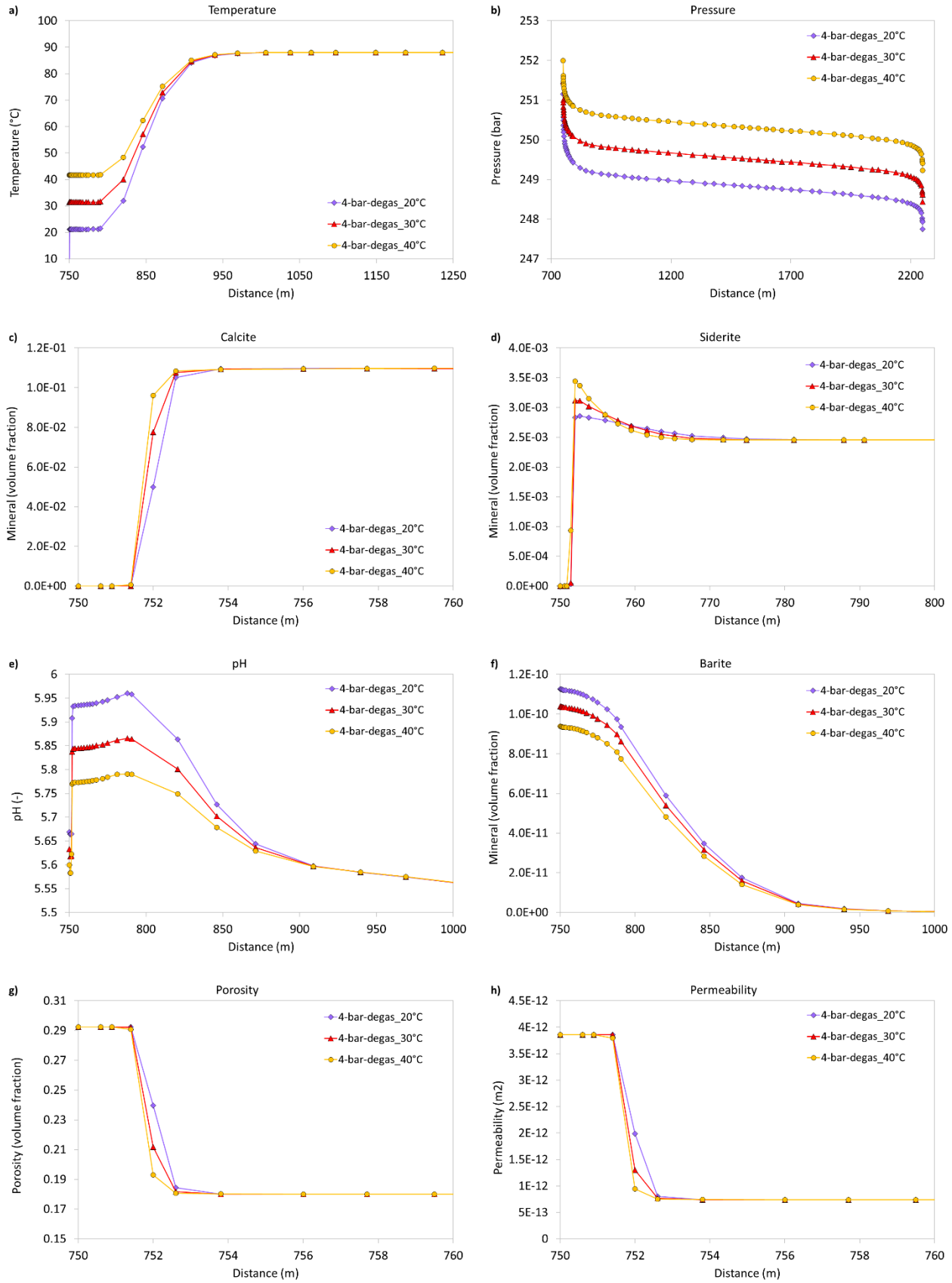

Figure 3: The simulation results of the three temperature scenarios are shown for the transect of 68 cells between the injection well left and the production well right (transect shown in fig. 2, upper). Note the different distances plotted for each variable. The figures show a) Temperature gradient. b) Pressure evolution. c) Calcite dissolution near-well. d) Siderite dissolution and precipitation. e) pH drop near-well and increase further in the cooled zone. f) Barite precipitation. g) Porosity increase near-well. h) Permeability increase near-well.

4.3.2 Simulation results for the CO_2 scenarios

The resulting temperature after 7 years of injection and production is similar for all scenarios, indicating no difference because of CO_2 reduction or addition (figure 4a). The difference in injected mass is expressed in the pressure response, with a higher pressure for more CO_2 injected (figure 4b). The base case of 4 bar degassing (1) has the lowest pressure. Scenario two of re-injecting CO_2 results in a slight <1 bar pressure increase and scenario three of CH_4-used CO_2 injection results in an ~1 bar pressure increase. However, the effect of injection temperature on the pressure is still larger for the first three scenarios, keeping the reservoir pressure below the initial value of 255 bar. Scenario four with maximum CO_2 co-injection on the other hand, shows significant pressure increase due to the added mass of CO_2. The pressure increase is 20 bar above the initial value of 255 bar (figure 4b).

All scenarios show similar dissolution and precipitation patterns of calcite and siderite dissolution and precipitation to the base case (figure 4a, figure 4b). However, calcite dissolution is clearly controlled by the CO_2 content of the water since higher CO_2 concentrations yield a more acidic injection fluid (figure 4e), which has a higher dissolution potential of calcite (figure 4c). This results in a more advanced calcite dissolution front for the CH_4-used CO_2 injection scenario two and especially the maximized CO_2 co-injection scenario four. The difference in calcite dissolution for different CO_2 concentrations is also observed for siderite (figure 4b). Besides enhanced dissolution, a higher CO_2 content also results in higher precipitation further in the reservoir due to increased transport of dissolved species. The carbonate dissolved zone has a low pH, lowest for the highest CO_2 content (figure 4e). Further in the reservoir, the pH is increased due to carbonate precipitation for the CO_2 re-injection scenario and the base case (CO_2 degassing) scenario. For the CH_4-used CO_2 injection scenario and especially the CO_2 co-injection scenario, their low initial pH values result in a pH in the precipitation zone that is, despite carbonate precipitation, still lower than the initial reservoir value. Barite precipitation is little affected by the CO_2 concentration, although slightly lower for the high CO_2 levels (figure 4f).

The porosity is dominantly controlled by calcite dissolution and shows an increase from 18% to 29%, stretching further into the reservoir when injecting a CO_2 richer solution (figure 4g). Although the final value of porosity and permeability increase is the same as for the thermal scenarios (figure 3h and figure 4h), the increased volume of permeability enhancement indicates that using CO_2 has a higher potential for stimulating the reservoir. After 7 years of injection, the current base case operations results in the emission of 1.33E+06 kg of CO_2 (table 9). The CO_2 addition scenario shows that 3.96E+08 could be stored in the reservoir after 7 years which is 1 megaton of CO_2 after 17 years.

Table 9: Change in CO_2 content of the reservoir after 7 years.

Scenario	**CO_2 added to or removed from the reservoir (kg)**
1. Base case (CO_2 degassing @ 4 bar)	-1.33E+06
2. CO_2 re-injection	0
3. CH_4-used CO_2 injection	1.24E+07
4. Maximized CO_2 co-injection	3.96E+08

5. DISCUSSION

The effect of injection temperature on fluid-rock interactions for the base case scenario, with CO_2 concentrations corresponding to gas separation a pressure of 4 bar, was investigated by batch experiments and reactive transport simulations. Both the experiment and simulations predict that the lower injection temperature in a geothermal doublet would induce calcite, and to a lesser extent siderite, dissolution in the near well zone of the injector. Dissolution of carbonates in the reservoir rock would result in an increased injectivity and a corresponding pressure decrease during water injection. Whether the injected fluid has a temperature of 20°C, 30°C or 40°C does not have a significant impact on the chemical reactions but does significantly change the density and pressure. The density effect was also found by Veldkamp et al. (2016). They modelled a decrease in injection temperature from 35 °C to 20 °C using ThermoCalc software. The simulations showed two effects: a reduced injection pressure caused by the increased density of the brine and an increased friction caused by the increased viscosity. It was concluded that the density effect is significant and greatly outweighs the negative effect of the increased viscosity.

The extent to which carbonate dissolution occurs in the reservoir and impacts the injectivity is limited if only the CO_2 is re-injected that is present after degassing the geothermal water at 4 bar. Injecting higher amounts of CO_2 with the cold injection fluid can significantly enhance the stimulation processes, with the added benefit of reducing CO_2 emissions from geothermal energy production. A negative side-effect of co-injecting additional CO_2 up to the solubility limit is the pressure increase in the reservoir. In a reservoir with closed boundary conditions, as simulated in the current study, the added mass of CO_2 results in a significant pressure increase. A maximum pressure increase, and therefore a maximum CO_2 co-injection, depends on the geomechanical strength of a reservoir, to prevent fracturing of the near well zone which could damage both the rock and the well. This requires a more detailed study, including the mechanical response of the reservoir to pressure changes. The mechanical response of the reservoir to calcite dissolution and potential pore-collapse is also not considered in this study. For implementation of the soft-stimulation technique and especially CO_2 addition, which has the largest effect, the legislation on CO_2 storage must be complied to. Also, it has to be considered that for higher CO_2 concentration the corroding effect of the brine may increase.

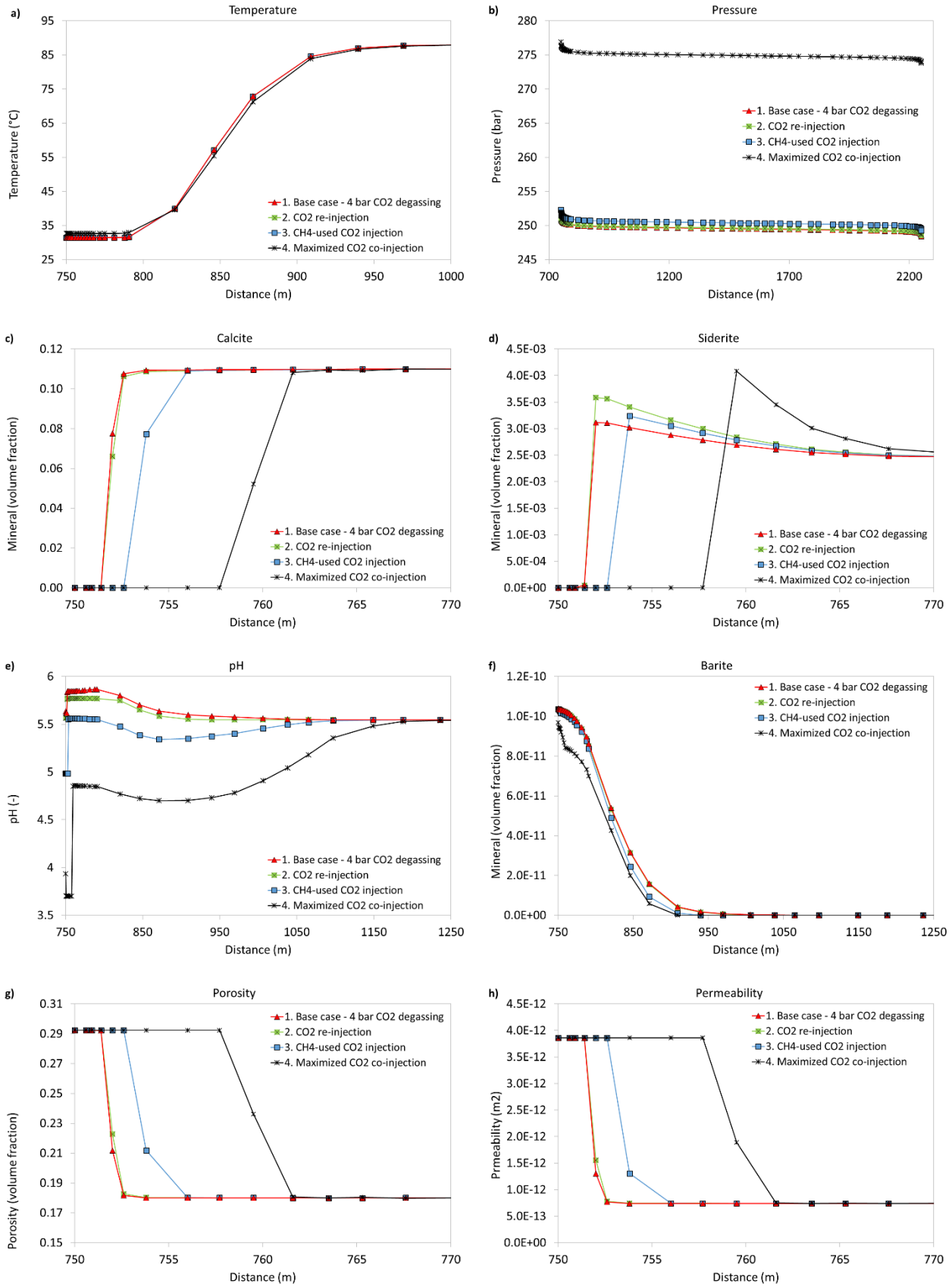

Figure 4: The simulation results of the four CO_2 content scenarios are shown for the transect of 68 cells between the injection well left and the production well right (transect shown in fig. 2). Note the different distances plotted for each variable. The figures show a) Equal cooling behaviour. b) Pressure evolution between the wells. c) Calcite dissolution near-well. d) Siderite dissolution and precipitation. e) Difference in pH due to different CO_2 concentrations. f) Similar barite precipitation. g) Porosity decrease mainly due to calcite dissolution. h) Permeability increase near-well.

Because geothermal operators experience injectivity decrease over time, in contrast to the predicted pressure decrease during cold water injection, other processes are probably affecting reservoir injectivity. The effect of counteracting mineral precipitation was studied, especially since the investigated stimulation techniques such as additional cooling may increase this process. Barite scaling has been reported as significant in geothermal systems (Orywall et al., 2017, Halidir and Balaban 2019) and could be a candidate for kinetically delayed precipitation in the reservoir, but the simulated amount of barite scaling is very low. However, the precipitation of barite that occurred during initialization of the formation water, indicates uncertainties in the modelled solubility of barite. There is also the possibility of other minerals forming which are currently not taken into account in the model. The experiment did show a strontium mineral forming and reduction in strontium concentration in the water. Experiments that are currently ongoing to help assess if reservoir precipitation is causing a permeability decline in the studied geothermal reservoir. The lack of a simulated injectivity decline could also indicate that other processes are involved which are not in the model, such as particle clogging (Ungemach, 2003, Gallup, 2009).

6. CONCLUSIONS

- Field-scale TOUGHREACT simulations were performed for a Dutch geothermal doublet. The simulation results indicate that soft stimulation of the reservoir by enhanced calcite (and siderite) dissolution could yield a large porosity increase from 18 to 29 %. Consequently, a considerable permeability improvement around the injection well could be possible of 750 mD to 3.75 D. This indicates that there is a potential for CO_2-content and temperature optimization to stimulate injectivity improvement.
- The different temperature scenarios show that increased cooling gives a higher potential for calcite dissolution. The difference in calcite dissolution for temperatures between 20°C and 40 °C is however small. The increase of fluid density with lower temperatures has a larger effect on reservoir pressure and injectivity.
- The different CO_2 re-injection scenarios indicate that increased CO_2 addition enhances calcite dissolution, increasing the potential for soft-stimulation of the reservoir. The technology has the additional benefit of reducing CO_2 emissions into the atmosphere.

ACKNOWLEGDEMENTS

This project has been subsidized through the ERANET Cofund GEOTHERMICA (Project no. 731117), from the European Commission, Topsector Energy subsidy from the Ministry of Economic Affairs of the Netherlands, Federal Ministry for Economic Affairs and Energy of Germany and EUDP.

REFERENCES

Alt-Epping, P., Waber, H., Diamond, L., and Eichinger, L.: Reactive transport modeling of the geothermal system at Bad Blumau, Austria: Implications of the combined extraction of heat and CO_2, *Geothermics*, **45**, (2013), 18-30.

Balen van, R., Van Bergen, F., De Leeuw, C., Pagnier, H., Simmelink, H., Van Wees, J., and Verweij, J.: Modelling the hydrocarbon generation and migration in the West Netherlands Basin, *the Netherlands. Netherlands Journal of Geosciences*, **79**(01), (2000), 29-44.

Blanc, Ph., Lassin, A., Piantone, P., Azaroual, M., Jacquement, N., Fabbri, A., Gaucher, E.C., Thermoddem: A geochemical database focused on low temperature water/rock interactions and waste materials, *Applied Geochemistry*, **27**, (2012), 2107-2116.

Blöcher, G., Reinsch, T., Henninges, J., Milsch, H., Regenspurg, S., Kummerow, J., and Huenges, E.: Hydraulic history and current state of the deep geothermal reservoir Groß Schönebeck, *Geothermics*, **63**, (2016), 27-43.

Boch, R., Leis, A., Haslinger, E., Goldbrunner, J. E., Mittermayr, F., Fröschl, H., and Dietzel, M.: Scale-fragment formation impairing geothermal energy production: interacting H_2S corrosion and $CaCO_3$ crystal growth, *Geothermal Energy*, **5**(1), (2017), art. no. 4.

Donselaar, M. E., Groenenberg, R. M., and Gilding, D. T.: Reservoir geology and geothermal potential of the Delft Sandstone Member in the West Netherlands Basin, *Paper presented at* World Geothermal Congress 2015, Melbourne, Australia (2015, April).

Gallup, D.L.: Production engineering in geothermal technology: A review, *Geothermics*, **38**(3), (2009),326-334.

Haklıdır, T.F.S., and Balaban, Ö.T.: A review of mineral precipitation and effective scale inhibition methods at geothermal power plants in West Anatolia (Turkey), *Geothermics*, **80**, (2019), 103-118.

Hesshaus, A., Houben, G., and Kringel, R.: Halite clogging in a deep geothermal well – Geochemical and isotopic characterisation of salt origin, *Physics and Chemistry of the Earth*, **Parts A/B/C**, **64**, (2013), 127-139.

Holmslykke, H. D., Kjøller, C., and Fabricius, I. L.: Core Flooding Experiments and Reactive Transport Modeling of Seasonal Heat Storage in the Hot Deep Gassum Sandstone Formation, *ACS Earth and Space Chemistry,* **1**(5), (2017), 251-260.

Hommel, J., Coltman, E., Class, H.: Porosity–Permeability Relations for Evolving Pore Space: A Review with a Focus on (Bio)geochemically Altered Porous Media, *Transport in Porous Media*, **124 (2)**, (2018), 589-629.

Huq, F., Haderlein, S. B., Cirpka, O. A., Nowak, M., Blum, P., and Grathwohl, P.: Flow-through experiments on water–rock interactions in a sandstone caused by CO_2 injection at pressures and temperatures mimicking reservoir conditions, *Applied Geochemistry*, **58**, (2015), 136-146.

Lasaga, A.C., Soler, J.M., Ganor, J., Burch, T.E., Nagy, K.L.: Chemical weathering rate laws and global geochemical cycles, *Geochimica et Cosmochimica Acta*, (1994), **58 (10)**, 2361-2386.

Orywall, P., Drüppel, K., Kuhn, D., Kohl, T., Zimmermann, M., and Eiche, E.: Flow-through experiments on the interaction of sandstone with Ba-rich fluids at geothermal conditions, *Geothermal Energy*, **5**(1), (2017), art. no. 20.

Palandri, J.L., Kharaka, Y.K.: A compilation of rate parameters of water-mineral interaction kinetics for application to geochemical modeling. U.S. Geological Survey, *Open File Report* 2004-1068.

Pruess, K.,: ECO2N: A TOUGH2 fluid property module for mixtures of water, NaCl, and CO_2. LBNL-57952, 2005.

Pruess, K., Oldenburg, C. and Moridis, G.: TOUGH2 User's Guide, Version 2.0. Report LBNL-43134. Lawrence Berkeley National Laboratory, Berkeley, CA (1999).

Regenspurg, S., Geigenmüller, I., Rybacki, E., and Milsch, H.: Redox Reactions During Sandstone Flow-through Experiments at Geothermal Conditions, *Procedia Earth and Planetary Science,* **17**, (2017), 53-56.

Schreiber, S., Lapanje, A., Ramsak, P., and Breembroek, G.: Operational issues in geothermal energy in Europe: Status and overview (2016).

Staatstoezicht op de Mijnen: Staat van de sector Geothermie. (2017). From https://geothermie.nl/images/Onderzoeken-en-rapporten/SvdSGeothermie.pdf

Ungemach, P.: Reinjection of cooled geothermal brines into sandstone reservoirs, *Geothermics*, **32**(4-6), (2003), 743-761.

Veldkamp, H., and Boxem, T.: Sector outlook: Geothermal power increase in the Netherlands by enhancing the capacity (TNO 2015 R11618). TNO. (2015).

Veldkamp, J.G., Loeve, D., Peters, E., Nair, R., Pizzocolo, F., and Wilschut, F.: Thermal fracturing due to low injection temperatures in geothermal doublets. (2016).

Verma, A., Pruess, K.: Thermohydrological conditions and silica redistribution near high-level nuclear wastes emplaced in saturated geological formations, *Journal of Geophysical Research*, **93 (B2)**, (1988), 1159-1173.

Wasch, L.J.: Geothermal Energy-Scaling potential with cooling and CO_2 degassing. TNO report. TNO 2013 R11661. (2014).

Xu, T., Sonnenthal, E., Spycher, N., Pruess, K.: TOUGHREACT – A simulation program for non-isothermal multiphase reactive geochemical transport in variably saturated geologic media: Applications to geothermal injectivity and CO_2 geological sequestration. *Computers and Geosciences*, 32, (2006), 145-165.